

# A Two-axis Bimorph Piezoelectric Actuator for Pressure and Slippage Force Presentation

Masahiro Ohka<sup>\*</sup>, Yasuhiro Sawamoto<sup>\*</sup>, Shiho Matsukawa<sup>\*</sup>, Tetsu Miyaoka<sup>\*\*</sup> and Yasunaga Mitsuya<sup>\*\*\*</sup>

<sup>\*</sup>Nagoya University, Graduate School of Information Science, Department of Complex Systems Science  
Furo-cho, Chikusa-ku, Nagoya, 464-8601, Japan

<sup>\*\*</sup>Shizuoka Institute of Science and Technology, Faculty of Science and Technology, Department of Information System  
Toyosawa 2200, Fukuroi, 473-8555, Japan

<sup>\*\*\*</sup>Nagoya University, Graduate School of Engineering, Department of Electro-Mechanical Engineering  
Furo-cho, Chikusa-ku, Nagoya 464-8603, Japan

## Abstract:

We are studying a two-axis micro-actuator to enhance the presentation reality of a tactile display that is capable of presenting pressure distribution and shearing force. We develop two types of actuators; Actuator A is composed of sequentially connected  $x$ - and  $y$ -directional actuators; each actuator is comprised of bimorph piezoelectric actuators. The  $x$ - and  $y$ -directional actuators are independently controlled by changing the applied voltage to position a probe that is attached to the tip of a two-axis actuator. The maximum displacement and force generated by the  $x$ -directional actuator are 1.1 mm and 0.03 N, respectively. Those generated by  $y$ -directional actuator are 1.0 mm and 0.06 N, respectively. Actuator B is composed of two bimorph actuators making an angle, two small links and three joints. At the present, we confirm that the actuator can move along  $x$  and  $y$ -axes of two-dimensional coordinate. Finally, since relationship between applied voltage and displacement caused by the voltage shows a hysteresis loop in the bimorph actuator used as components of the two-axis actuator, we produce a control system for the two-axial actuator based on a multi-layered artificial neural network to compensate the hysteresis.

## 1. INTRODUCTION

In order to enhance the presentation reality of a tactile display [1]-[6], pressure distribution and shearing force should be presented simultaneously on a display pad, because there are pressure and shearing force acceptance points (mechanoreceptive units) that are distributed on human palm and finger surfaces. Thus, we are studying a two-axis micro-actuator to develop a tactile display pad that comprises two-axis actuators. Since the size of each actuator used in the array should be miniaturized because of the need for high distribution density on the stimulus points of the display pad, we adopt a bimorph piezoelectric actuator as a basic part of the two-axis actuator.

We developed two types of two-axis of actuator A and B. Actuator A is composed of sequentially connected  $x$ - and  $y$ -directional actuators that are both comprised of two bimorph piezoelectric actuators connected in parallel to each

other. Actuator B is composed of two bimorph piezoelectric actuators making an angle, two small links and three joints. We developed a testing machine composed of laser displacement detectors, a two-axial actuator, and an  $x$ - $y$  stage to test the two-axial actuator. We simultaneously evaluated the effects of presenting normal and tangential stimuli according to results of our psychophysical experiments. Since relationship between applied voltage and displacement caused by the voltage shows a hysteresis loop in the bimorph actuator used as components of the two-axial actuator, we produce a control system for the two-axis actuator based on a multi-layered artificial neural network to compensate the hysteresis.

## 2. RESEARCH OVERVIEW AND ORGANIZATION

At this time, several researchers have examined the tactile recognition mechanism of the human hand in detail using microneurography [7] and psychophysical experimentation [8] [9]. Microneurography is a method of examining a reaction to a given stimulus via signals sensed by a tungsten microelectrode that is inserted into a nerve fiber. Psychophysical experiments involve methods of examining a human subject's replies to questions regarding the strength of a stimulus. These studies used these types of experimental methods to reach several conclusions. The mechanoreceptive units of human tactile organs are known as the Fast Adapting type I unit (FA I), the Fast Adapting type II unit (FA II), the Slowly Adapting type I unit (SA I), and the Slowly Adapting type II unit (SA II). FA II can perceive a mechanical vibration of 0.2  $\mu$  m in amplitude. FA I or FA II can perceive a surface unevenness of 3  $\mu$  m in amplitude. SA I can perceive a pattern formed with Braille dots.

When designing tactile displays, we should develop an actuator that is capable of controlling several microns of vibration superimposed upon about a 1 mm displacement. As we require a dynamic range of 1/1000 for the actuator and no-backlash, the usual electric motors are insufficient for satisfying actuator specifications.

In this paper, we adopt the piezoelectric effect as a principle of the present actuator, since not only the bimorph

piezoelectric actuator can generate displacement of about 1 mm, it also has no backlash. We attempt to develop a tactile display comprised of two-axis actuators that are capable of generating pressure and slippage force.

We require micro machining-measurements to develop the two-axial actuator. Moreover, evaluating the present tactile display requires psychological evaluation. Thus, in the Japan Scientific Research of Priority Area 438, the “Next-Generation Actuators Leading Breakthroughs”, Y. Mitsuya takes charge of the micro machining-measurements and T. Miyaoka oversees the psychological evaluation. Research representative M. Ohka takes charge of the design and development of the tactile display.

### 3. HUMAN TACTILE SENSING CAPABILITY

In order to estimate the advantages of the present actuator on the tactile display, Miyaoka obtained human psychophysical thresholds for normal and tangential vibrations on the hand. Miyaoka measured the vibrotactile thresholds at the distal pad of the left index finger by transmitting tangential-sinusoidal vibrations onto the skin surface with a small contactor. Seven subjects took part in this experiment. The tangential stimuli were transmitted with a contactor 2.5 mm in diameter. We attached the contactor to a vibrator (AKASHI, MEE-025) that was assembled to produce tangential vibrations.

The subject sat down, and then placed his/her left hand on the contactor. Tangential vibrations were transmitted to the distal pad of the subject’s left index finger. We changed the stimuli amplitudes using the PEST procedure [10]. For each subject, we took four measurements for each stimulus frequency.

We calculated the average tangential thresholds obtained for the seven subjects with a 2.5 mm contactor. The average tangential-threshold curve is shown in Fig. 1. The open circles in the figure denote the average thresholds. The threshold curve decreased linearly from 4 to 50 Hz, increased gently until 100 Hz, and decreased again above 100 Hz. We observed a U-shaped curve between 100 and

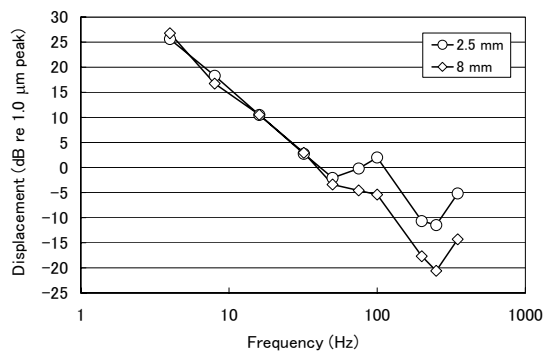


Fig. 1 Shearing force threshold depending on contact-area

350 Hz. The shape of the tangential-threshold curve indicates that at least two types of mechanoreceptors determine the shape of the curve. Based on previous studies [7][8], FA II is believed to be the mechanoreceptor above 100 Hz.

Below 100 Hz, determining the participating mechanoreceptor became difficult. The exponent of the power function, fitted to the thresholds between 4 and 50 Hz, was  $-1.22$ . Exponents of the power functions became approximately  $-1$  and  $-2$  when the participating mechanoreceptors were FA I and FA II, respectively. The exponent of the present experiment differs from both values.

The tangential-threshold curves obtained with a 8 mm contactor are shown in Fig. 1. Open diamonds denote the tangential thresholds obtained with a 8 mm contactor. The two threshold curves overlapped between 4 and 50 Hz and were U-shaped, but they did not overlap between 100 and 350 Hz. The overlapping parts indicate that the same type of mechanoreceptor contributed to producing the curve slopes. Miyaoka suggested that the slowly adapting type II unit (SA II) contributed to determining the shapes of tangential-threshold curves [8].

Figure 2 shows the normal- and tangential-threshold curves. Open squares and open circles in the figure denote normal and tangential thresholds, respectively. The normal- and tangential-threshold curves were similar when the stimulus frequencies were between 100 and 350 Hz. These curves were U-shaped and we believe that FA II was the participating mechanoreceptor. When the stimulus frequencies were below 100 Hz, the slopes of normal and tangential curves developed differently from each other. The exponents of the power functions fitted to the two curves were  $-0.74$  and  $-1.22$  for the normal and tangential thresholds, respectively. The normal and tangential thresholds showed statistically significant differences at 4, 8, and 50 Hz (4 Hz,  $t = -5.15$ ,  $p < 0.01$ ; 8 Hz,  $t = -4.46$ ,  $p < 0.01$ ; 50 Hz,  $t = 2.77$ ,  $p < 0.05$ ). We consider the tangential slope,  $-1.22$ , to be similar to the SA II slope, while we consider the normal slope,  $-0.74$  to be similar to the FA I slope. These results suggest that SA II is the mechanoreceptor that contributes to

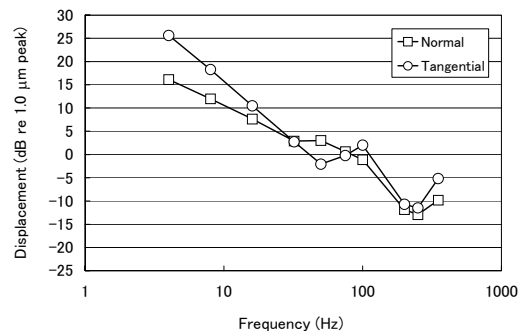


Fig. 2 Vibrotactile threshold depending on vibration direction

producing the shape of the tangential-threshold curves below 100 Hz.

#### 4. DEVELOPMENT OF TWO AXIAL ACTUATOR

Since the normal and tangential stimuli are essential for tactile presentation as shown in the previous chapter, we have made progress in the design of two-axis actuators that are composed of bimorph piezoelectric actuators. We describe a testing machine, Actuator A and B in the following sections.

##### 4.1 Testing Machine

Besides the development of the actuator, we have developed a testing machine to test the two-axis actuator, as shown in Fig. 3. And we developed an evaluation machine composed of laser displacement detectors, the two-axial actuator, and an  $x$ - $y$  stage.

Using the testing machine, we performed experiments for the voltage versus displacement under a free-ending condition, and obtained the relationship between displacement and force under a constant voltage condition. In the latter experiment, we tried to decrease the displacement toward zero by means of the  $x$ - $y$  stage under voltages of 50, 100, 150, and 200 V.

##### 4.2 Actuator A

Figure 4 shows type A actuator. This actuator is comprised of  $x$ -directional actuator of twin bimorph piezoelectric actuators and  $y$ -directional actuator of a single piezoelectric actuator connected to the  $x$ -directional actuator.

Figure 5 displays the present experimental results. The  $x$ - and  $y$ -directional relationships between force and displacement are superimposed in Fig. 5. The displacement generated in the zero-force condition also shows the

free-ending in Fig. 5. Both the  $x$ - and  $y$ -directional displacements generated in the zero-force condition are at about 1 mm. The generated force that increases with decreasing the displacement reaches its maximum at the zero-displacement condition. These variations in the generated force are approximated by linear equations.

When we compare the  $x$ -directional characteristic with the  $y$ -directional one, we notice that the inclination obtained from the  $y$ -directional characteristic is two times larger than the one obtained from the  $x$ -directional characteristic. This is because the  $x$ -directional actuator's stiffness is about 1/2 of the  $y$ -directional actuator's. This result means that different strengths between the  $x$ - and  $y$ -directional shearing forces are caused when the present actuator is applied to the tactile display. Thus, we are attempting to improve the actuator.

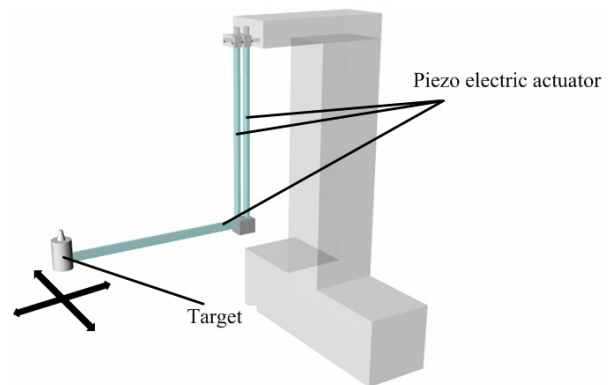


Fig.4 Two-axis actuator (type A)

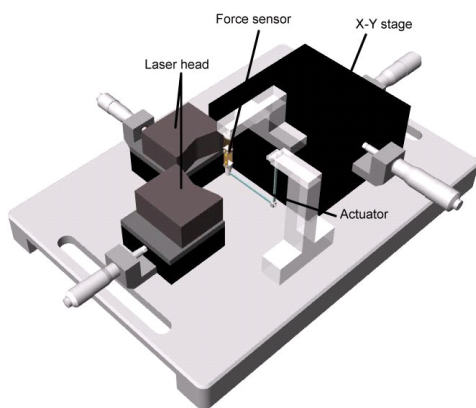


Fig.3 Testing machine for evaluation of the two-axis actuator

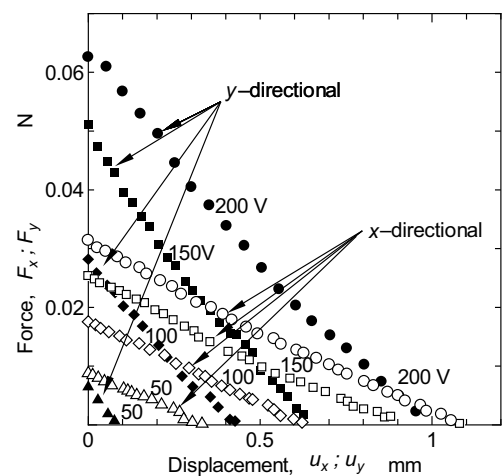


Fig. 5 Characteristics for the present two-axis actuator (type A)

### 4.3 Actuator B

The two-axis actuator as shown in Fig. 6 is composed of two bimorph actuators making an angle, two small links and three joints. This actuator is developed to enhance the stiffness of the  $x$  and  $y$ -directional actuators. Each bimorph piezoelectric actuator is independently controlled by change in applied voltage to position two-dimensionally a probe of the two-axis actuator.

Figure 7 shows trajectories of the tips or the two-dimensional actuator. As shown in Fig. 7, the actuator can move in the two-dimensional coordinate. However, these trajectories fluctuating around coordinate axis lines designated as input trajectories to the two-axis actuator. We are continuing to improve the present two-axis actuator.

### 6. CONTROL OF TWO AXIS ACTUATOR USING NEURAL NETWORK MODEL

Since the piezoelectric actuator has hysteresis, sensor feedback is required to generate precise displacement. However, it is difficult to amount displacement sensors on every actuator because a large amount of actuators are needed for the tactile display. A sensor-less mechanism is pursued to make the actuator array simple.

In this paper, we adopt a neural network model capable of learning hysteresis characteristics of the actuator as an estimator of generated displacement. Figure 8 shows the neural network [11] composed of four input neurons, 10 neurons in a hidden layer and a output neuron. The network is taught desired output signals according to error back propagation algorithm. In this network, the output neuron emits time derivative of displacement  $du/dt$ . Two neurons of the input layer show loading or unloading. One of the input layer and the other show current values of voltage and displacement. Therefore, preceding two components of

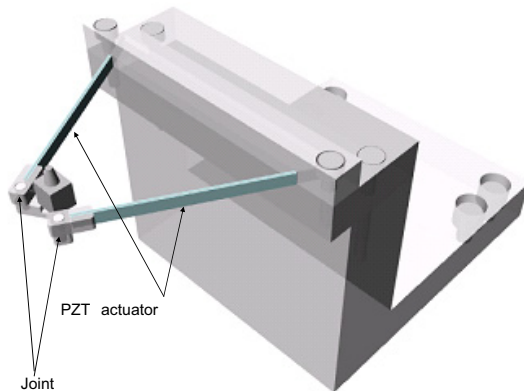


Fig.6 Two-axis actuator (type B)

input vector at loading and unloading are shown by  $(1, 0, V, u)$  and  $(0, 1, V, u)$ , respectively. Where,  $V$  and  $u$  are applied voltage and the current displacement, respectively. The displacement at next time increment is obtained by integrating the time derivative of displacement emitted by the output neuron.

In the learning experiment, a hysteresis loop containing minor loops is learned as desired data. Figure 9 shows comparison between the simulated and experimental results. As shown in Fig. 9, simulated relationship between input voltage and can estimate experimental results.

### 7. CONCLUSION

In order to enhance the presentation capability of the tactile display, we developed new two-axis actuators that are used for an actuator array of the tactile display. Simultaneously, according to the results of our psychophysical experiments, we evaluated the effects of presenting normal and tangential stimuli. Since relationship between applied voltage and displacement caused by the voltage shows a hysteresis loop in the bimorph actuator used as components of the two-axis actuator, we produce a control system for the two-axis actuator based on a multi-layered artificial neural network to compensate the hysteresis. Simulated result coincides with the experimental hysteresis.

In the future work, we will incorporate the new two-dimensional actuators into the tactile display. Then we will evaluate the tactile display with virtual object handling test and virtual texture recognition test.

### ACKNOWLEDGEMENT

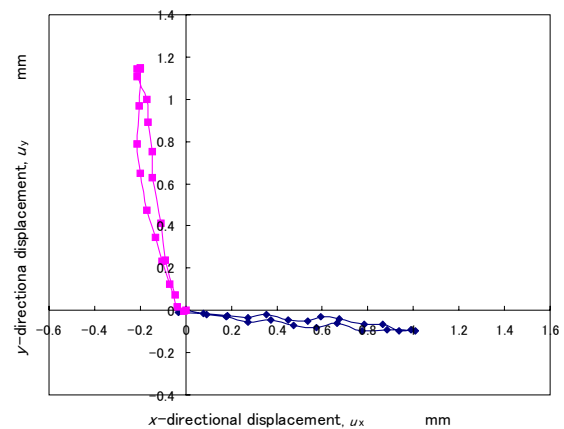


Fig.8 Trajectories of two-axis actuator (type B)

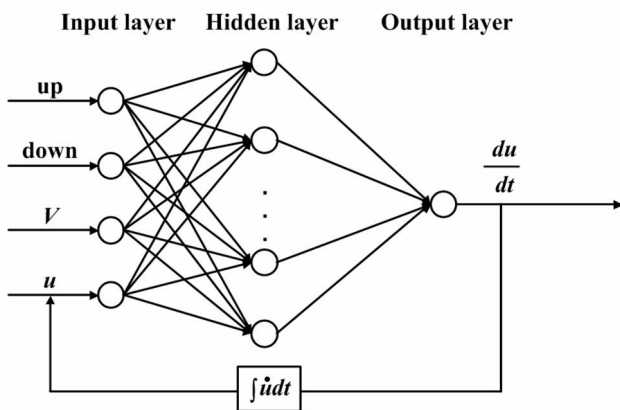


Fig.8 Neural network model including a feed back loop

This study was supported by fiscal 2005 grants from the Ministry of Education, Culture, Sports, Science and Technology (Grant-in-Aid for Scientific Research in Priority Areas, No. 1607807) and 2004 grant from the Tateisi Science and Technology Foundation.

#### REFERENCES

[1] Y. Ikei, M. Yamada, and S. Fukuda: Tactile Texture Presentation by Vibratory Pin Arrays Based on Surface Height Maps, Proc. of Int. Mechanical Engineering Conf. and Exposition, (1999), 51-58

[2] M. Takahashi, T. Nara, S. Tachi, and T. Higuchi: A Tactile Display Using Surface Acoustic Wave, Proc. of the 2000 IEEE Inter. Workshop on Robot and Human Interactive Communication, (2000), 364-367

[3] Y. Tanaka, H. Yamauchi, and K. Amemiya: Wearable Haptic Display for Immersive Virtual Environment, Fifth JFPS Inter. Symposium, (2002), 309-310

[4] PHANTOM, [http://www.sensable.com/products/phantom\\_ghost](http://www.sensable.com/products/phantom_ghost)

[5] Braille Cells, <http://www.kgs-jpn.co.jp/epiezo.html>

[6] M. Ohka, K. Kato, T. Fujiwara, and Y. Mitsuya, Virtual Object Handling Using a Tactile-haptic Display

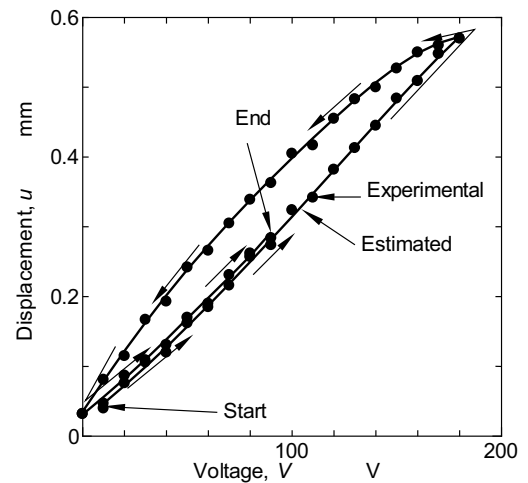


Fig.9 Comparison between simulated result of the neural network model and the experimental result

System, The Inter. Conf. on Mechatronics and Automation, (2005), 292-297

[7] S. J. Bolanowski, G. A. Gescheider, R. T. Verrillo, and C. M. Checkosky, Four channels mediate the mechanical aspects of touch, *Journal of the Acoustical Society of America*, **84** (1988), 1680-1694

[8] T. Miyaoka, Measurements of detection thresholds presenting normal and tangential vibrations on human glabrous skin, Proceedings of the Twentieth Annual Meeting of the International Society for Psychophysics, **20** (2004), 465-470

[9] T. Miyaoka, Mechanoreceptive mechanisms to determine the shape of the detection-threshold curve presenting tangential vibrations on human glabrous skin, Proceedings of the 21st Annual Meeting of The International Society for Psychophysics, **21** (2005), 211-216

[10] M. M. Taylor, & C. D. Creelman, "PEST: Efficient Estimate on Probability Functions", The Journal of the Acoustical Society of America, **141** (1967), 782-787

[11] David E. Rumelhart, Geoffrey E. Hinton and Ronald J. Williams, Learning representation by back-propagating errors, *Nature* **323**(1986), 533-536